Mechanism of Diffusion Slowdown in Confined Liquids

Hiroki Matsubara* and Fabio Pichierri

Department of Applied Chemistry, Graduate School of Engineering, Tohoku University and JST-CREST, Aoba-yama 6-6-07, Sendai 980-8579, Japan

Kazue Kurihara†

WPI-Advanced Institute for Materials Research (AIMR), Tohoku University and JST-CREST, 2-1-1 Katahira, Sendai 980-8577, Japan

(Received 12 July 2012; published 7 November 2012)

With the aid of molecular dynamics simulation, we consider why the diffusivity of liquid becomes slower as the liquid is confined to a narrower space. The diffusion coefficient of octamethylcyclotetrasiloxane liquid confined between two mica surfaces was calculated for a range of surface separations from 64 to 23 Å. The resulting separation dependence of the diffusion coefficient can be explained by considering that the molecular diffusion is an activated process. In particular, we find that the increase in the activation energy is closely correlated with the decrease of the potential energy per molecule, from which we propose a molecular-level mechanism of this confined-induced diffusion slowdown.

DOI: 10.1103/PhysRevLett.109.197801 PACS numbers: 68.15.+e, 66.10.C−, 83.10.Mj

In recent decades, different experimental techniques, particularly using the surface forces apparatus, have been developed so as to measure the change in the transport properties (i.e., viscosity and diffusion coefficient) of liquids from the macroscopic (bulk) regime down to states confined between two flat surfaces characterized by thicknesses of a few molecular diameters. These experiments have revealed that for most liquids, the viscosity increases (e.g., octamethylcyclotetrasiloxane [OMCTS] [1–5], liquid crystal [3], water [6], polymers [7], and ionic liquid [8]) or, equivalently, the diffusion coefficient decreases [9] by several orders of magnitude with respect to the corresponding bulk values. Molecular simulations also support this trend for the Lennard-Jones (LJ) molecules [10], water [11–13], and hydrocarbons [14,15]. Our aim in this Letter is to understand the microscopic mechanism of this confinement-induced slowdown, which is an important step towards the theoretical prediction and design of the liquid properties at nanosized spaces.

Microscopic insights into the properties on confined liquids have been brought by molecular simulation. OMCTS, a globular and nonpolar molecule, has played a central role as a typical liquid that forms a molecular layer structure parallel to the confining surface [16,17]. Several simulation studies where a simple model of the OMCTS molecule represented by a sphere in conjunction with the LJ potential were carried out to investigate the microscopic orders in the confined liquid as well as its correlation with the solvation force and the liquid properties [10,18]. These studies showed that the fine structural details of the confining surfaces and the liquid molecule sensitively affect the ordering, and therefore, the liquid properties, of the confined liquid. Therefore, it is necessary for a realistic model to properly take into account these atomic level details. Recently, we developed such a model for OMCTS liquid confined between two cleaved mica surfaces [19,20]. In our previous study, this model was employed to clarify the microscopic details of the confined OMCTS liquid by the molecular dynamics (MD) simulation where our attention was devoted to a single surface separation ($H = 57$ Å) corresponding to a 7 molecular layers state [20].

Here, we extend the range of separations, H, to $23 \leq H \leq 64$ Å, which correspond to 3–7 molecular layers states, in order to investigate how confinement slows down the liquid dynamics in terms of the diffusion coefficient. In particular, a correlation between the diffusion coefficient and potential energy is sought from the point of view of the activated diffusion (AD), from which we propose a molecular-level mechanism of the confinement-induced diffusion slowdown.

The AD is a common model for the diffusion of lattice defects [21], which is also applied to other condensed phases or molecular systems as long as a molecule spends a relatively long time being trapped inside a potential energy well formed by the neighboring molecules [22,23]. The effective depth, $E_a(\geq 0)$, of the potential well is called the activation (free) energy. The molecule sometimes surmounts E_a by thermal fluctuations, and migrates to a nearby potential well. Thus, the diffusion process is composed of successive migrations, and the diffusion coefficient, D, is proportional to the rate of migration as $D = Ce^{-\beta E_a}$, where $\beta = 1/(k_B T)$, k_B is Boltzmann's constant, and T is the absolute temperature. Here C is a constant; therefore, any possible effect of confinement is included in E_a. In the following, we apply the AD to our confined liquid. As is explicitly indicated by the density distribution which has a layered structure [20], the confined liquid considered here displays a spacial nonuniformity which is originated by the contact with the solid surfaces, thereby the activation energy can be a function

of the position, $\mathbf{r}$. Correspondingly, we introduce the local activation energy, $E_a^{\mathrm{loc}}(\mathbf{r})$, defined as the activation energy necessary to be surmounted for a molecule to migrate from $\mathbf{r}$ to a nearby potential well.

From the microscopic description of the AD, it is likely that $E_a^{\mathrm{loc}}(\mathbf{r})$ is correlated with the local potential energy that a molecule feels at $\mathbf{r}$, $\varepsilon^{\mathrm{loc}}(\mathbf{r})$. Following this line, we partition $E_a^{\mathrm{loc}}(\mathbf{r})$ as $E_a^{\mathrm{loc}}(\mathbf{r}) = -\varepsilon^{\mathrm{loc}}(\mathbf{r}) + \alpha^{\mathrm{loc}}(\mathbf{r})$, where $\alpha^{\mathrm{loc}}(\mathbf{r})$ describes the remaining effects other than that of the potential energy. Most of them are expected to be thermal effects, such as the configurational change that occurs during the migration, of molecules composing the potential well around $\mathbf{r}$. The activation energy of the total system is given by a spacial average over the system volume, Ω: $E_a = \frac{1}{\Omega}\int_\Omega E_a^{\mathrm{loc}}(\mathbf{r})d\mathbf{r} = -\varepsilon + \alpha$, where $\varepsilon = \frac{1}{\Omega}\int_\Omega \varepsilon^{\mathrm{loc}}(\mathbf{r})d\mathbf{r}$ and $\alpha = \frac{1}{\Omega}\int_\Omega \alpha^{\mathrm{loc}}(\mathbf{r})d\mathbf{r}$. Although at this stage, the partition of E_a into ε and α represents an assumption of our model, later on we will show that here the separation dependence of α is weak in comparison with that of ε and the following simple approximation

$$E_a(H) \sim -\varepsilon(H) + \text{const.}, \tag{1}$$

reasonably describes the separation dependence of the diffusion coefficient.

MD simulation is used to investigate the correlation between E_a and ε. The diffusion coefficient and ε were calculated by changing the surface separation in the range $23 \le H \le 64$ by 1 Å step. The computational details of and procedures adopted in the present MD simulation are same as those in the previous study except for the range of H, and a detailed description can be found in Ref. [20]. An overview of our MD system is shown in Fig. 1. DL_POLY 2 (version 2.20) software package [24] was used. The system configuration is based on the liquid-vapor coexistence method proposed by Leng [25]. Thousand hundreds OMCTS molecules are confined by the mica surface with a surface area of 81.8×81.2 Å. A repulsive wall expressed by harmonic potentials was added at the edge of mica surfaces. These were put in a fixed orthorhombic simulation box of $400 \times 81.2 \times 110$ Å with the 3D periodic boundary conditions, and the system temperature was set to 300 K by using a Nose-Hoover thermostat [26]

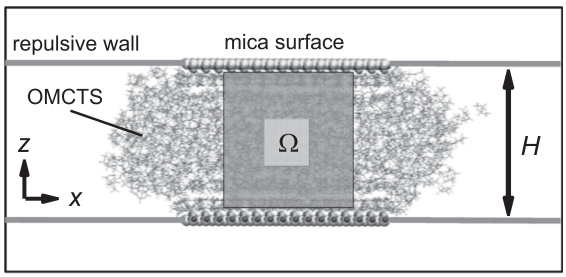

FIG. 1. View of our MD system. Molecules within a fixed slit volume Ω are included in the statistics.

(NVT ensemble). Any motion of the mica surface was kept frozen while each OMCTS molecule was approximated by a rigid body whose equation of motion was numerically integrated by Fincham's implicit quaternion algorithm [27] with a time step of 2 fs. Liquid-liquid and liquid-surface interactions are modeled by the LJ type interaction sites located on each position of the C atom of OMCTS, and O and K^+ atoms of mica. For all these LJ potentials, a cutoff radius of 10 Å was used. At each surface separation, the system was equilibrated for more than 1 ns, followed by a production run of 4 ns with a data storage interval of 1 ps. In the calculation of physical properties, only the molecules inside Ω, which is defined by $|x| < 20$, were included in the statistics. This strategy avoids any possible effect of the edges along the x direction.

The diffusion coefficient was calculated from the root mean square deviation (RMSD) of the molecular center of mass position $\mathbf{R}$: $D_{\mathrm{RMSD}} = \lim_{t\to\infty}\frac{1}{6t}\langle[\mathbf{R}(t) - \mathbf{R}(0)]^2\rangle$, where $\langle\ldots\rangle$ means the ensemble average.

The potential energy per molecule was calculated based on a spacial mesh division. We assigned $\varepsilon_I = 1/2\sum_{J\neq I} u_{IJ}$ to molecule I, where u_{IJ} is the pair interaction energy between molecule I and J. The slit volume Ω was divided into small 3D meshes of size $dx \times dy \times dz = 1.0 \times 1.0 \times 0.1$ Å. The local potential energy per molecule at mesh i was calculated as $\varepsilon_i^{\mathrm{loc}} = \langle\varepsilon_{I\in i}\rangle$, which was then averaged over Ω: $\varepsilon = \frac{1}{N_m}\sum_{i=1}^{N_m}\varepsilon_i^{\mathrm{loc}}$, where N_m is the total number of meshes (If a mesh was not visited by any molecule during the simulation, the mesh was excluded from the average).

The separation dependence of the diffusion coefficient calculated by the MD simulation, D_{RMSD}, is shown as a solid curve in Fig. 2(a) (left axis). D_{RMSD} decreases by 2 orders of magnitude, from 0.193×10^{-9} m^2/s at $H = 64$ Å, which is comparable to the bulk value of 0.256×10^{-9} m^2/s [19], to 0.0007×10^{-9} m^2/s at $H = 23$ Å. This result is not far from the experimental observations of Mukhopadhyay *et al.* by the fluorescence correlation spectroscopy [9] that the diffusion coefficient at $H = 30$ Å is about 2 orders less than the bulk value. The force curve calculated from the MD simulation is shown in Fig. 2(b). The period of oscillation is ~8 Å, which is consistent with the experimental results [2,17]. Checking the density profile in z direction, we confirmed that this range of H corresponds to states made of from approximately 3 to 7 molecular layers as is noted in Fig. 2(b). While the diffusion curve shows no significant discontinuity so as to imply a first-order phase transition, an oscillatory behavior, which is inversely correlated with that of the force curve, can be seen for the separations less than $H = 35$ Å corresponding to the transition from 5 to 4 molecular layers. Our MD result here is among others consistent with the atomic force microscopy results of Maali *et al.* [28] where the viscosity increased with an oscillation whose period was 7.8 Å.

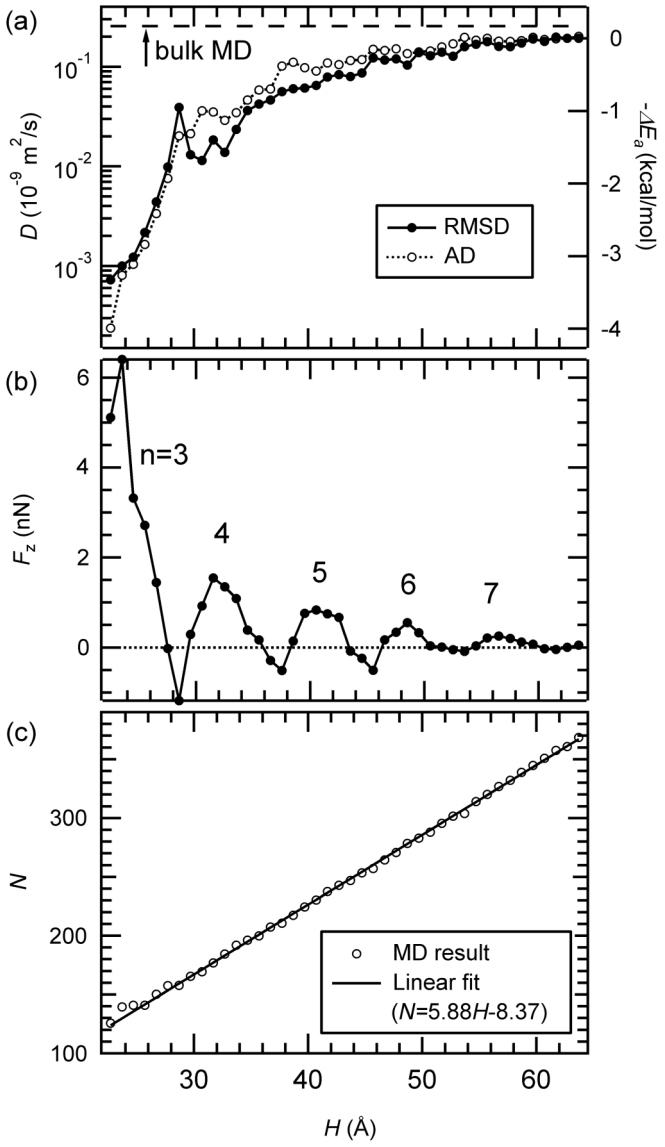

FIG. 2. The separation dependence of physical properties. (a) The diffusion coefficient calculated from the RMSD is compared with the prediction from the activated diffusion (AD) model (left axis), as well as the corresponding activation energy change from the value at $H_0 = 64$ Å (right axis). The dashed line shows the bulk value; (b) z component of force acting on mica surface (an average of upper and lower surface); (c) number of molecules in the slit volume Ω. The solid line corresponds to a linear fitting.

Now we investigate the relation between the diffusion coefficient and the potential energy per molecule. If Eq. (1) holds, the AD predicts the diffusion coefficient as $D_{\mathrm{AD}}(H) = D_{\mathrm{RMSD}}(H_0)e^{\beta\Delta\varepsilon(H)}$, where $\Delta\varepsilon(H) = \varepsilon(H) - \varepsilon(H_0)$, using $D_{\mathrm{RMSD}}(H_0)$ and $\varepsilon(H_0)$ at an arbitrary reference surface separation H_0. As shown in Fig. 2(a), left axis, D_{AD} thus predicted (with the choice $H_0 = 64$ Å) shows a good correlation with D_{RMSD}, which indicates that the potential energy makes the dominant contribution to the activation energy. We notice that the peak at 29 Å in D_{RMSD} is not reproduced in D_{AD}. Also, the agreement is good for H larger than ~55 Å where the liquid has a diffusivity which is comparable to the bulk value. This fact implies that the view of the migration dynamics is kept valid by the short-lived potential well made by the neighbors which are quickly moving around. The right axis of Fig. 2(a) shows the diffusion slowdown in terms of the activation energy difference $\{-\Delta E_a(H) = -[E_a(H) - E_a(H_0)]$ for D_{RMSD} while $\Delta\varepsilon(H)$ for $D_{\mathrm{AD}}\}$. ε at $H_0 = 64$ Å was calculated as -8.5 kcal/mol. One order drop in the diffusion coefficient corresponds to ~1.4 kcal/mol drop in the activation energy, and the depth of potential well becomes 3–4 kcal/mol deeper associated with the separation change from $H = 64$ to 23 Å. The diffusion coefficient parallel to the surface, D_{xy}, is often of interest [10–14]. We found that the dependence of D_{xy} on H is similar to that of D_{RMSD} (see the Supplemental Material [29]). Therefore, at least in our system, the D_{AD} also gives a good approximation to D_{xy}.

Why does the confinement decrease the potential energy? We begin by investigating the liquid density, whose increase makes the diffusion slower. Unfortunately, H has an uncertainty of several angstroms due to the unclear boundary between the confining solid and the confined liquid. It is thereby difficult to know the true value of the average density in the slit, $\bar{\rho}$, which is proportional to N/H, where N is the average number of molecules inside the slit. Instead, we observe that N decreases almost linearly with H as shown in Fig. 2(c) except for the small oscillation about the line. The linear decrease in N can be similarly seen in other molecular liquids (LJ, hexadecane, tetracosane, and squalane) [30] although, there, the oscillation may be larger than in our case. The linear fit leads to $N = 5.88H - 8.37$. If necessary, we can replace H by $H' = H + 8.37/5.88$ within the uncertainty of H to make N/H constant. From these considerations, we conclude that the average density here is in effect invariant with respect to the change of H.

While the average density is kept constant, the local density does change; i.e., the entropy changes depending on H. Actually, on the basis of thermodynamic considerations it can be qualitatively shown that the decrease of the potential energy is closely related to the entropy reduction. Consider an isothermal shrink process of the separation from $H + \Delta H$ (state 0) and H (state 1) as shown in Fig. 3. The slit volume Ω is divided into two constant volume regions, A and B, by hypothetical planes parallel to the surface through which a molecule can freely pass. Volume B is exactly squeezed out by the shrink process, i.e., the height of B is ΔH. Below, internal energy, number of molecules, entropy are denoted as U, N, S, respectively; subscript distinguishes region A or B; superscript distinguishes state 0 or 1 if the variable takes different values depending on state 0 or 1; Δ means the variation associated with the shrink process. Being based on the MD result,

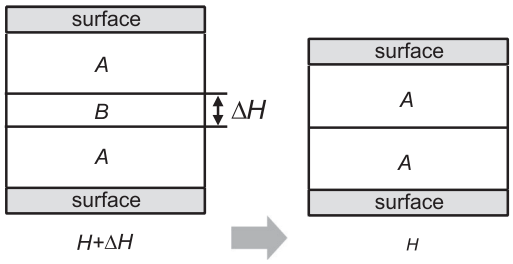

FIG. 3. Hypothetical division of the slit volume Ω.

we assume $N \propto H$, from which $\Delta N_A = 0$ results. The change of the potential energy per molecule in Ω is $\Delta\varepsilon = U_A^1/N_A - (U_A^0 + U_B^0)/(N_A + N_B) = \Delta U_A/N_A - \varepsilon_{AB}^0 N_B/(N_A + N_B)$, where $\varepsilon_{AB}^0 = U_B^0/N_B - U_A^0/N_A$ is the difference in the potential energy per molecule between A and B at state 0 (The difference per molecule of internal energy is equivalent to that of potential energy due to the isothermal condition). The thermodynamic relationship regarding region A leads to $\Delta U_A = \Delta W_A + T\Delta S_A + \mu\Delta N_A = T\Delta S_A$, where μ is the chemical potential and ΔW_A is the work done on volume A by the shrink process. $\Delta W_A = 0$ because both the surface and the volume of A do not change. From these relations, finally we find that

$$\Delta\varepsilon = T\Delta S_A/N_A - \varepsilon_{AB}^0 N_B/(N_A + N_B). \qquad (2)$$

The first term indicates the entropy decrease resulting from the prohibition of some statistical configurations by the geometrical constraint. On the other hand, the second term arises by the squeezing out of molecules having higher potential energy, because a molecule in region A has lower potential energy by the stronger attractive interaction with the solid surface than that in region B; i.e., $\varepsilon_{AB} \geq 0$ typically holds. The decrease of the potential energy per molecule thus induced by the confinement leads to an increase of the activation barrier for diffusion through Eq. (1), and the diffusion coefficient decreases. This is a possible scenario suggested for the confinement-induced diffusion slowdown. It should be noted that the effect of confinement is well isolated in this system because the temperature and the average density, which also cause a diffusion slowdown, are constant.

In this Letter, based on a realistic molecular simulation, we showed that the confined-induced diffusion slowdown can be well understood if one considers the molecular diffusion to be a thermally activated process. The picture that emerges from this activated diffusion seems to be valid not only for the solidlike or glasslike states but also for liquidlike states. The simple expression of the activation energy seen here [Eq. (1)], possibly thanks to the near-ideal molecular properties of OMCTS, is a good starting point when considering more general cases. For example, in the confined dodecane films, the formation of crystalline bridges drastically decreases the diffusion coefficients [14]. Testing if the activated diffusion can explain such a complicated behavior will lead to finding more general expressions of the activation energy which would provide a comprehensive picture of the liquid confinement physics. Also, this study would be helpful in shedding light on the controversial problem of the confined-induced solidification in OMCTS liquid: discontinuous changes in the slowdown are observed in some experiments [2,3] whereas in other experiments [4,5,31] these changes are more gradual.

This research is supported by the Core Research for Evolutional Science and Technology (CREST) program of the Japan Science and Technology Agency (JST). We thank Dr. Bill Smith (Daresbury Laboratory) and the CCP-5 project for a copy of the DL_POLY molecular simulation package.

*matsubara@che.tohoku.ac.jp
†Also at Institute of Multidisciplinary Research for Advanced Materials (IMRAM), Tohoku University, 2-1-1 Katahira, Sendai 980-8577, Japan.

[1] S. Granick, Science **253**, 1374 (1991).
[2] J. Klein and E. Kumacheva, Science **269**, 816 (1995).
[3] M. Mizukami, K. Kusakabe, and K. Kurihara, Prog. Colloid Polym. Sci. **128**, 105 (2004).
[4] T. Becker and F. Mugele, Mol. Simul. **31**, 489 (2005).
[5] L. Bureau, Phys. Rev. Lett. **104**, 218302 (2010).
[6] H. Sakuma, K. Otsuki, and K. Kurihara, Phys. Rev. Lett. **96**, 046104 (2006).
[7] P. M. McGuiggan, M. L. Gee, H. Yoshizawa, S. J. Hirz, and J. N. Israelachvili, Macromolecules **40**, 2126 (2007).
[8] K. Ueno, M. Kasuya, M. Watanabe, M. Mizukami, and K. Kurihara, Phys. Chem. Chem. Phys. **12**, 4066 (2010).
[9] A. Mukhopadhyay, J. Zhao, S. C. Bae, and S. Granick, Phys. Rev. Lett. **89**, 136103 (2002).
[10] J. Gao, W. D. Luedtke, and U. Landman, Phys. Rev. Lett. **79**, 705 (1997).
[11] Y. Liu, Q. Wang, and L. Lu, Langmuir **20**, 6921 (2004).
[12] P. Liu, E. Harder, and B. J. Berne, J. Phys. Chem. B **108**, 6595 (2004).
[13] S. R.-V. Castrillón, N. Giovambattista, I. A. Aksay, and P. G. Debenedetti, J. Phys. Chem. B **113**, 1438 (2009); J. Phys. Chem. B **113**, 7973 (2009).
[14] A. Jabbarzadeh, P. Harrowell, and R. I. Tanner, J. Chem. Phys. **125**, 034703 (2006); Tribol. Int. **40**, 1574 (2007).
[15] S. T. Cui, P. T. Cummings, and H. D. Cochran, J. Chem. Phys. **114**, 7189 (2001).
[16] J. N. Israelachvili, *Intermolecular and Surface Forces* (Academic Press, London, 2011), 3rd ed.
[17] R. G. Horn and J. N. Israelachvili, J. Chem. Phys. **75**, 1400 (1981).
[18] K. G. Ayappa and R. K. Mishra, J. Phys. Chem. B **111**, 14 299 (2007).
[19] H. Matsubara, F. Pichierri, and K. Kurihara, J. Chem. Theory Comput. **6**, 1334 (2010).
[20] H. Matsubara, F. Pichierri, and K. Kurihara, J. Chem. Phys. **134**, 044536 (2011).

[21] H. Mehrer, *Diffusion in Solids: Fundamentals, Methods, Materials, Diffusion-Controlled Processes* (Springer, NewYork, 2007).
[22] M. Goldstein, J. Chem. Phys. **51**, 3728 (1969).
[23] E. M. Calvo-Mũnoz, M. E. Selvan, R. Xiong, M. Ojha, D. J. Keffer, D. M. Nicholson, and T. Egami, Phys. Rev. E **83**, 011120 (2011).
[24] W. Smith, Mol. Simul. **32**, 933 (2006).
[25] Y. Leng, J. Phys. Condens. Matter **20**, 354 017 (2008).
[26] S. Nosé, Prog. Theor. Phys. Suppl. **103**, 1 (1991).
[27] D. Fincham, Mol. Simul. **8**, 165 (1992).
[28] A. Maali, T. Cohen-Bouhacina, G. Couturier, and J.-P. Aimé, Phys. Rev. Lett. **96**, 086105 (2006).
[29] See Supplemental Material at http://link.aps.org/supplemental/10.1103/PhysRevLett.109.197801 for the results of the separation dependence of the parallel and perpendicular diffusion coefficients.
[30] J. Gao, W. D. Luedtke, and U. Landman, J. Phys. Chem. B **101**, 4013 (1997).
[31] A. L. Demirel and S. Granick, Phys. Rev. Lett. **77**, 2261 (1996).